

# Role of GADD45A in myocardial ischemia/reperfusion through mediation of the JNK/p38 MAPK and STAT3/VEGF pathways

YANG WANG<sup>1-3</sup>, HUI GAO<sup>1-3</sup>, XIANGHONG CAO<sup>1-3</sup>, ZHENG LI<sup>1-3</sup>, YE KUANG<sup>1-3</sup>, YONG JI<sup>1-3</sup> and YI LI<sup>1-3</sup>

<sup>1</sup>Department of Clinical Laboratory, Yan'an Hospital Affiliated to Kunming Medical University;

<sup>2</sup>Key Laboratory of Tumor Immunological Prevention and Treatment of Yunnan Province;

<sup>3</sup>Key Laboratory of Biotherapy of Kunming City, Kunming, Yunnan 650051, P.R. China

Received June 7, 2022; Accepted September 5, 2022

DOI: 10.3892/ijmm.2022.5200

**Abstract.** Rapid recovery of blocked coronary artery blood flow after myocardial infarction (MI) is the key to reducing the size of the infarcted area, improving clinical outcome and decreasing mortality. However, ischemia/reperfusion (I/R) injury has a complicated pathological mechanism and is an inevitable complication of coronary artery blood flow recovery. Growth arrest and DNA damage-inducible  $\alpha$  (GADD45A) serves a vital role in myocardial injury induced by I/R. The present study aimed to explore the role and mechanisms of GADD45A in cardiac microvascular endothelial cells (CMEC)-I/R injury *in vivo* and *in vitro*. An I/R injury rat model and a hypoxia/reoxygenation (H/R) cellular model were established, and myocardial tissues were collected for GADD45A detection, 2,3,5-triphenyltetrazolium chloride staining, H&E staining, and dual staining of CD31 and TUNEL. Serum was also collected for the analysis of creatine kinase and lactate dehydrogenase in I/R rats following GADD45A silencing. Additionally, the protein expression levels of CD31, phosphorylated-endothelial nitric oxide synthase (p-eNOS), endothelin-1 (ET-1), JNK, p38 MAPK, STAT3 and VEGF were assessed by western blotting. The JNK and p38 MAPK activator, anisomycin, and the JAK2-STAT3 pathway inhibitor, AG490, were used to determine the involvement of JNK/p38 MAPK pathway and STAT3/VEGF pathway. GADD45A was highly expressed in I/R injury rat and cell models. GADD45A silencing reduced the ischemic area and improved myocardial pathological damage *in vivo*. Furthermore, the levels of CD31 and p-eNOS were increased, whereas ET-1 was decreased by GADD45A silencing in the I/R injury rats. Mechanistically, GADD45A silencing reduced JNK/p38 MAPK expression

but activated STAT3/VEGF expression. GADD45A silencing inhibited H/R-induced viability reduction and apoptosis through MAPK signaling and suppressed angiogenesis via STAT3/VEGF in H/R-induced CMECs. Overall, GADD45A ameliorated apoptosis and functional injury of CMECs via the JNK/p38 MAPK and STAT3/VEGF pathways.

## Introduction

It has been reported that inflammation induced by ischemia/reperfusion (I/R) injury mainly occurs in non-cardiac cells, such as leukocytes, fibroblasts and endothelial cells (1). When I/R injury occurs, cardiac microvascular dysfunction results in reduced oxygen supply to cardiac cells (2). Current treatments for myocardial infarction (MI) are based on two principles: Short-term revascularization and long-term angiogenesis (3,4). Short-term revascularization, such as coronary artery bypass grafting or percutaneous coronary intervention, are widely used for treatment (3). However, the beneficial effects of revascularization are limited owing to low myocardial microvascular density and poor local perfusion at the infarct margin (5,6). Moreover, it has been demonstrated that changes in capillary bed structure after I/R injury may lead to reduced microcirculation flow (7).

Cardiac microvascular endothelial cells (CMECs) are the most common cells in the heart and are the basic components of myocardial microcirculation; under normal conditions, CMECs can secrete cytokines related to cardiac growth, contractile performance and rhythm (8). In addition, a previous study highlighted the role of CMEC dysfunction in driving I/R injury in cardiomyocytes (9). It was also reported that the sustained viability, the reduced apoptosis and the increase in nitric oxide (NO) generation in CMECs after I/R injury could alleviate myocardial I/R injury (10,11). Therefore, attenuating CMEC injury may be able to protect against myocardial I/R-induced injury. A recent study reported that growth arrest and DNA damage-inducible  $\alpha$  (GADD45A) expression was increased in ischemic myocardial cells and could be targeted by microRNA (miR)-1283 to reduce hypoxia/reoxygenation (H/R)-induced apoptosis of myocardial cells (12). Nevertheless, its expression in CMECs remains unknown.

GADD45A was found to be distributed in endothelial cells of myocardial tissue in the Human Protein Atlas database (13),

**Correspondence to:** Professor Yi Li, Department of Clinical Laboratory, Yan'an Hospital Affiliated to Kunming Medical University, 245 Renmin East Road, Kunming, Yunnan 650051, P.R. China  
E-mail: lyliyi227@163.com

**Key words:** myocardial ischemia reperfusion, growth arrest and DNA damage-inducible  $\alpha$ , JNK/p38 MAPK pathway, STAT3/VEGF pathway, CD31 cardiac microvascular endothelial cells

but its expression in endothelial cells of H/R-treated myocardial tissue is unknown. Thus, we hypothesized that GADD45A may be involved in the pathogenesis of MI by affecting the apoptosis and angiogenesis of CMECs. Therefore, the present study aimed to explore whether GADD45A participated in the apoptosis and dysfunction of CMECs following myocardial I/R injury.

## Materials and methods

**Animal model.** Male Sprague-Dawley rats (SPF grade; age, 6 weeks; weight, 180–220 g;  $n=30$ ) were fed under standard laboratory conditions with a temperature of 27°C, 40–60% humidity and 12-h light/dark cycle. The rats were acclimated to these conditions for 7 days and provided with free access to water and food. The rats were then anesthetized with 1% pentobarbital sodium (30 mg/kg) by intraperitoneal (i.p.) injection, and the myocardial I/R model was established following the surgical protocol of a previous study (10). A total of 21 rats were successfully induced in the I/R model with a survival rate of 91.3% (21/23), which was similar to previous studies (14,15); ischemia time may be the cause of death of two rats. All rats were randomly divided into 4 groups ( $n=7$  rats/group): i) Control group (Sham operation), in which open heart surgery was performed but the anterior descending branch of the coronary artery was not ligated; ii) I/R group; iii) I/R + lentiviral short hairpin-RNA-NC (Lv-sh-NC) group; and iv) I/R + Lv-sh-GADD45A group. Lentiviral vectors containing shRNA targeting GADD45A (Lv-sh-GADD45A, 5'-CGCAGAGCAGAAGATCGAAAG-3') and the Lv-sh-NC (5'-TTCTCCGAACGTGTCACGT-3') were constructed by Hanbio Biotechnology Co., Ltd. During ligation, 20  $\mu$ M lentivirus vectors ( $4 \times 10^9$  IFU/ml) were injected into the pericardial tissue of rat hearts at four different places around the infarcted area. No obvious side effects were found following I/R surgery and administration of si-GADD45A.

At 7 days post-I/R surgery, the rats were anesthetized with 1% pentobarbital sodium (30 mg/kg; i.p.) and rapid thoracotomy was performed. Blood (10 ml) was collected from the apex of the heart and serum was separated by first letting the collected blood stand at 37°C for 30 min, and then centrifuged at  $1,006 \times g$  at 4°C for 15 min to detect the levels of creatine kinase (CK), lactate dehydrogenase (LDH) and NO (described below). Next, the rats were euthanized by the i.p. injection of 1% pentobarbital sodium (150 mg/kg) and pre-cooled saline was injected into the apex of the heart through an intravenous infusion device for irrigation. Cessation of breathing for 3 min was used to verify death. After full irrigation, the quickly separated heart was washed in saline, placed on ice and dried with absorbent paper. The myocardial tissue was collected for 2,3,5-triphenyltetrazolium chloride (TTC) staining and other experiments, as described below.

Animal experiments were approval of the animal care and ethics committee of Yan'an Hospital Affiliated to Kunming Medical University (Kunming, China) and performed following the ARRIVE guidelines (<https://www.nc3rs.org.uk/arrive-guidelines>). The humane endpoints considered in this experiment were as follows: i) The animals showed mental depression accompanied by hypothermia ( $<37^\circ\text{C}$ ) in the absence of anesthesia; ii) the experiments were terminated

before the earliest indicator if an animal experienced severe pain. Any animals reaching these endpoints were to be euthanized with 1% pentobarbital sodium (150 mg/kg; i.p.).

**Reverse transcription-quantitative PCR (RT-qPCR).** Total RNA was extracted from myocardial tissues or CMECs using TRIzol® (Invitrogen; Thermo Fisher Scientific, Inc.) according to the manufacturer's instruction. cDNA was synthesized from the total RNA using the PrimeScript™ RT Reagent kit (cat. no. RR037A; Takara Bio, Inc.) according to the manufacturer's instructions. qPCR was conducted using the SYBR® Premix EX Taq™ kit (Takara Bio, Inc.) and the following thermocycling conditions: Initial denaturation for 5 min at 94°C; followed by 40 cycles of denaturation for 20 sec at 94°C, annealing for 20 sec at 65°C and elongation for 30 sec at 70°C. The following primer sequences were used: Rat GADD45A forward, 5'-TAAGCAAGAAGCCGGAAGA-3' and reverse, 5'-GGGTCTACGTTGAGCAGCTT-3'; human GADD45A forward, 5'-CGAAAGGATGGATAAGGTG-3' and reverse, 5'-GGATCAGGGTGAAGTGGGA-3'; GAPDH (rat) forward, 5'-TGTGAACGGATTTGGCCGTA-3' and reverse, 5'-GATGGTGATGGGTTTCCCGT-3'; and GAPDH (human) forward, 5'-GCACCGTCAAGGCTGAGAAC-3' and reverse, 5'-GGATCTCGCTCCTGGAAGATG-3'. mRNA expression levels were quantified using the  $2^{-\Delta\Delta C_q}$  method and normalized to the internal reference gene GAPDH (16).

**Western blotting.** Total proteins were isolated from rat myocardial tissue and cell samples using RIPA (Beyotime Institute of Biotechnology) and semi-quantified using a BCA kit (Beyotime Institute of Biotechnology). Proteins (20  $\mu$ g/lane) were separated on 12% gels by SDS-PAGE and transferred to PVDF membranes (cat. no. FFP24; Beyotime Institute of Biotechnology). PVDF membranes were blocked with 5% skimmed milk at room temperature for 2 h and then incubated at 4°C overnight with primary antibodies against: GADD45A [1:1,000; cat. no. 4632; Cell Signaling Technology, Inc.(CST)], CD31 (1:1,000; cat. no. ab281583; Abcam), phosphorylated (p)-eNOS (1:1,000; cat. no. bs-3589R; BIOSS), eNOS (1:1,000; cat. no. ab300071; Abcam), endothelin-1 (ET-1; 1:1,000; cat. no. ab2786; Abcam), p-p38 MAPK (1:1,000; cat. no. bs-5476R; BIOSS), p38 MAPK (1:1,000; cat. no. bs-0637R; BIOSS), p-JNK (1:1,000; cat. no. 4668; CST), JNK (1:1,000; cat. no. 9252; CST), early growth response 1 (EGRI; 1:1,000; cat. no. 4154; CST), p-STAT3 (1:1,000; cat. no. ab32143; Abcam), STAT3 (1:1,000; cat. no. ab68153; Abcam), VEGF (1:1,000; cat. no. 19003-1-AP; Proteintech Group, Inc.), BCL2 (1:1,000; cat. no. ab196495; Abcam), Bax (1:1,000; cat. no. ab32503; Abcam), cleaved caspase 3 (1:1,000; cat. no. 9661; CST) and GAPDH (1:10,000; cat. no. ab181602; Abcam). Subsequently, the membranes were incubated with HRP-conjugated goat anti-rabbit (1:2,000; cat. no. ab6721; Abcam) or goat anti-mouse (1:2,000; cat. no. ab6789; Abcam) secondary antibodies at 4°C for 1 h. BeyoECL Plus (Beyotime Institute of Biotechnology) was used to visualize the protein bands, and densitometric analysis was conducted using ImageJ 1.8.0 software (National Institutes of Health).

**TTC staining.** The heart slices (1.5 mm) were firstly placed in TTC solution (Sigma-Aldrich; Merck KGaA) with pH of 7.4 at

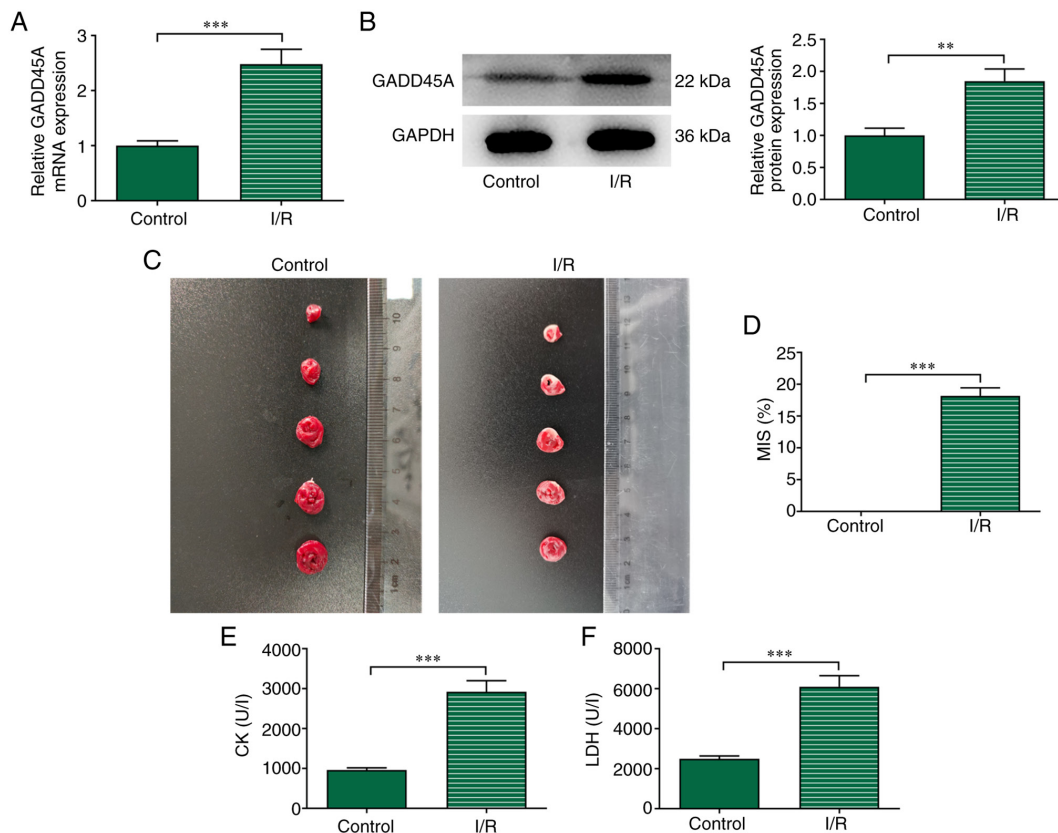


Figure 1. GADD45A expression is increased in I/R-induced myocardial tissues. (A) mRNA and (B) protein expression levels of GADD45A in myocardial tissues after I/R treatment. (C) TTC staining of rat hearts. (D) Myocardial infarct size. The levels of (E) CK and (F) LDH in serum.  $n=7$ ; \*\* $P<0.01$ , \*\*\* $P<0.001$ . CK, creatine kinase; GADD45A, growth arrest and DNA damage-inducible  $\alpha$ ; I/R, ischemia/reperfusion; LDH, lactate dehydrogenase; MIS, myocardial infarct size; TTC, 2,3,5-triphenyltetrazolium chloride.

37°C for 15 min, and then fixed in 4% paraformaldehyde for 24 h at room temperature. The color of the normal myocardium became red, and that of the ischemic myocardium was gray. The MI area was calculated using an EOS 90D digital camera (Canon, Inc.) to capture images and the staining was quantified by ImageJ2x software (National Institutes of Health).

**Measurement of CK, LDH and NO levels.** Serum (100  $\mu$ l) was used to determine the contents of LDH (Beyotime Institute of Biotechnology) and CK (Sigma-Aldrich; Merck KGaA) in rats according to the manufacturer's protocols. NO level in the serum was detected using an NO kit (cat. no. S0021S; Beyotime Institute of Biotechnology) in line with the kit instructions. CK, LDH and NO levels were examined using a CHEMIX-180 automatic biochemistry analyzer (Sysmex Corporation).

**H&E staining.** The myocardial tissues were fixed in 4% paraformaldehyde at room temperature. After 12 h, the tissues were dehydrated in an ascending gradient of ethanol and then made transparent with xylene. Next the tissues were embedded in paraffin wax and sliced into 4- $\mu$ m-thick sections. Finally, the sections were stained with hematoxylin for 5 min at 4°C and then with eosin for 3 min at 4°C. H&E staining was observed under a BX43 light microscope (Olympus Corporation).

**Immunofluorescence staining.** Cardiac tissues and CMECs were fixed with 4% paraformaldehyde at room temperature for 12 h and for 20 min, respectively, and then permeabilized

with 0.5% Triton X-100 at room temperature for 5 min. The 5- $\mu$ m-thick sections and CMECs were blocked with 5% normal goat serum (Beijing Solarbio Science & Technology Co., Ltd.) for 1 h at room temperature, incubated at 4°C overnight with primary antibodies against CD31 (1:1,000; cat no. 28083-1-AP; Proteintech Group, Inc.) and subsequently incubated with goat anti-rabbit Alexa Fluor® 488 IgG secondary antibody (1:100; cat. no. ab150077; Abcam) or goat anti-rabbit Alexa Fluor® 555 IgG secondary antibody (1:200; cat. no. ab150078; Abcam) at 37°C for 1.5 h in the dark. At least five randomly selected fields were examined using an IX73 inverted fluorescence microscope (Olympus Corporation).

**TUNEL assay.** Rat hearts were fixed at room temperature for 24 h in 4% paraformaldehyde and dehydrated with 30% sucrose at room temperature for 24 h. Subsequently, the hearts were embedded in paraffin and then sliced into 4-5  $\mu$ m sections. Apoptotic cells in the heart tissues were stained using a One-step TUNEL Apoptosis Detection kit (cat. no. C1086; Beyotime Institute of Biotechnology) in accordance with manufacturer's protocol and observed under an IX73 inverted fluorescence microscope (Olympus Corporation).

**Cell culture.** Human CMECs were purchased from BLUEFBIO, and HUVECs were from American Type Culture Collection; both were incubated in Dulbecco's Modified Eagle Medium supplemented with 10% FBS (both from HyClone; Cytiva) in an incubator containing 5% CO<sub>2</sub> at 37°C.

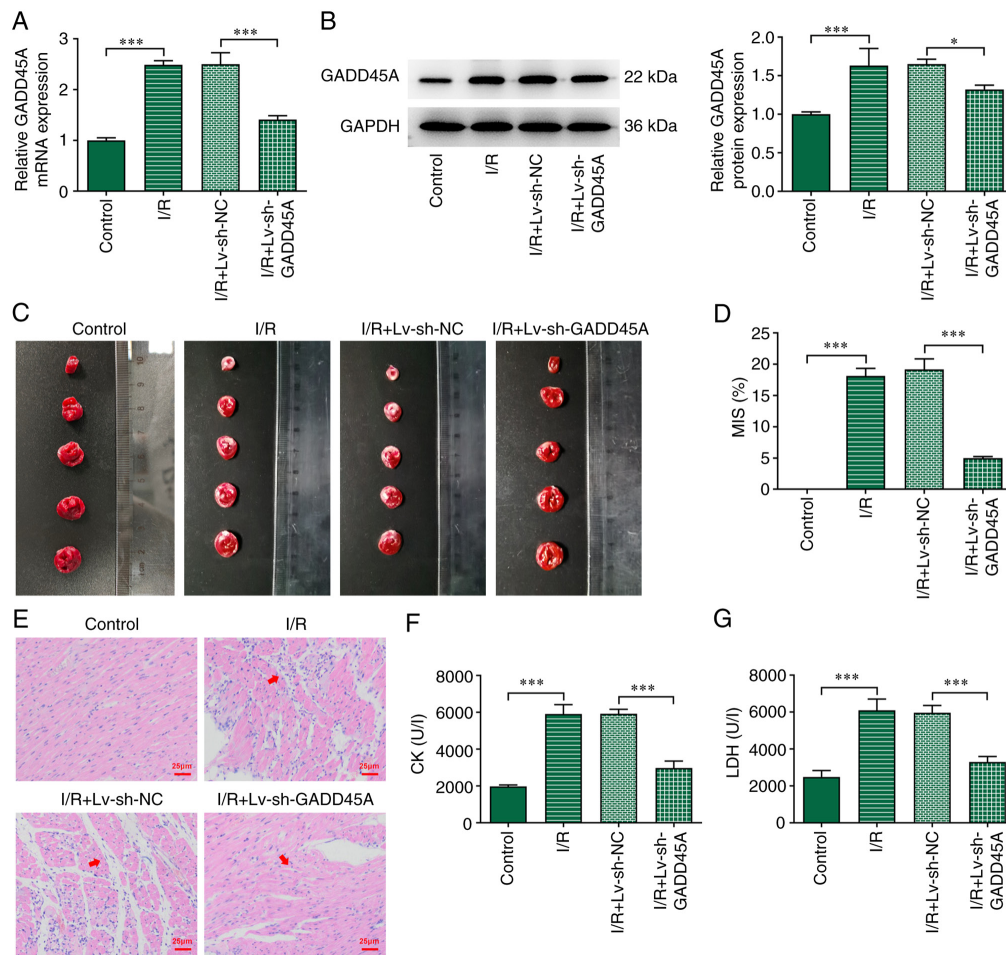


Figure 2. Effects of GADD45A silencing on myocardial pathology. (A) mRNA and (B) protein expression levels of GADD45A in heart tissues showing the transfection efficacy of Lv-si-GADD45A on I/R-induced rats. (C) TTC staining of rat hearts. (D) Myocardial infarct size. (E) H&E staining. Levels of (F) CK and (G) LDH in serum.  $n=7$ ; \* $P<0.05$ , \*\*\* $P<0.001$ . CK, creatine kinase; GADD45A, growth arrest and DNA damage-inducible  $\alpha$ ; I/R ischemia/reperfusion; Lv, lentivirus; LDH, lactate dehydrogenase; MIS, myocardial infarct size; NC, negative control; si, small interfering RNA; TTC, 2,3,5-triphenyltetrazolium chloride.

**H/R cell model and transfection.** Plasmids inducing GADD45A silencing (siRNA-GADD45A-1 and -2; siB08722144103-1-5 and siB08722144126-1-5, respectively; 80 nM; Guangzhou RiboBio Co., Ltd.) or an siRNA-NC (siN00000002-1-5; 80 nM) were transfected into human CMECs using Lipofectamine® 2000 (Invitrogen; Thermo Fisher Scientific, Inc.) for 48 h at 37°C following the standard procedures of the manufacturer. After 48 h, the transfected cells were incubated in a hypoxic incubator (95%  $N_2$  and 5%  $CO_2$ ) at 37°C for 45 min and then under normoxic conditions (21%  $O_2$ , 5%  $CO_2$  and 74%  $N_2$ ) at 37°C for 90 min, then used for subsequent experimentation.

In rescue experiments, prior to H/R induction, CMECs were treated with the JNK and p38 MAPK activator, anisomycin (5  $\mu$ M), or with an inhibitor of STAT3, AG490 (50  $\mu$ mol/l), for 2 h at 37°C.

**Cell Counting Kit-8 (CCK-8) viability assay.** CMEC viability in each group was detected using the CCK-8 kit (Nanjing Jiancheng Bioengineering Institute) according to the manufacturer's protocol. A total of  $2 \times 10^4$  cells/well were seeded into 96-well plates for 24 h at 37°C. Then, 10  $\mu$ l CCK-8 solution was added to each well and the cells were incubated for further

2 h at 37°C. Finally, a microplate reader was used to assess the absorbance at  $\lambda=450$  nm.

**Flow cytometry.** CMECs were cultured in 6-well plates ( $1 \times 10^6$  cells/well) for 24 h at 37°C. The apoptotic level of CMECs in each group was assessed by Annexin V/FITC-PI Apoptosis Detection kit (Beyotime Institute of Biotechnology) according to the manufacturer's protocol. Total apoptotic rates (equal to early-plus late-stage apoptosis) were analyzed using a CytoFLEX flow cytometer with FlowJo v10 software (FlowJo; BD Biosciences).

**Tube formation.** Matrigel (50  $\mu$ l) was spread into 96-well plates at 37°C for 30 min. After H/R treatment for 30 min at 37°C, 100  $\mu$ l HUVECs ( $2 \times 10^5$  cell/ml) were added to each well. To confirm the role of JAK2-STAT3 pathway in angiogenesis, JAK2-STAT3 pathway inhibitor AG490 was added. Angiogenesis was observed after 6 h incubation at 37°C under a BX43 light microscope (Olympus Corporation).

**Statistical analysis.** All experiments were repeated at least three times. Data are presented as the mean  $\pm$  SD and analyzed with GraphPad Prism v7.0 (GraphPad Software; Dotmatics).

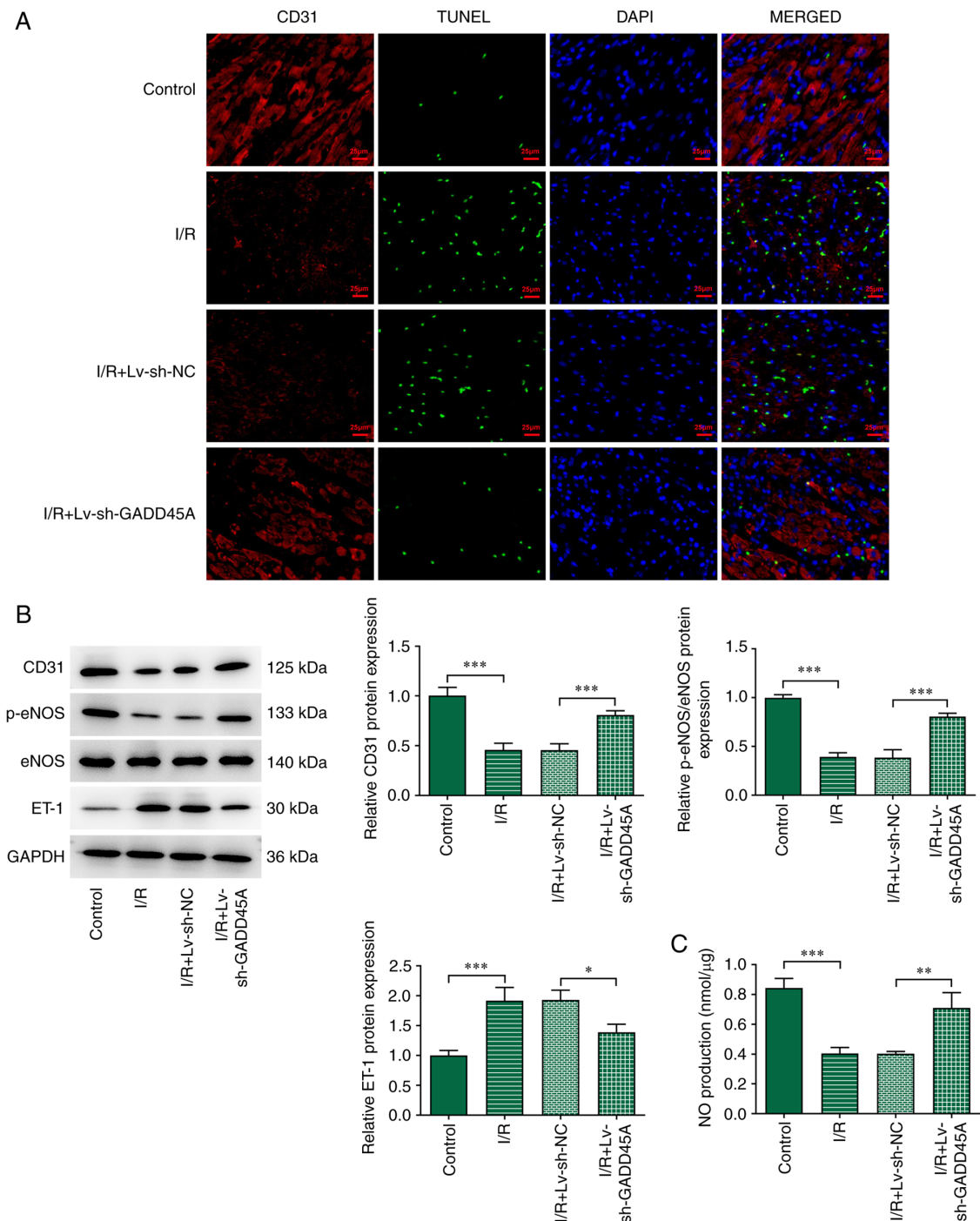


Figure 3. Effects of GADD45A on vascular endothelial cell loss. (A) Dual-staining of CD31 and TUNEL in I/R model rats with or without Lv-si-GADD45A treatment; DAPI was used to stain the nuclei. (B) CD31, p-eNOS, eNOS and ET-1 expression levels were examined by western blotting. (C) NO serum levels were detected using an NO kit. Each experiment was repeated at least three times. \* $P < 0.05$ , \*\*\* $P < 0.001$ . eNOS, endothelial NO synthase; ET-1, endothelin-1; GADD45A, growth arrest and DNA damage-inducible  $\alpha$ ; I/R ischemia/reperfusion; Lv, lentivirus; NC, negative control; NO, nitric oxide; p-, phosphorylated; si, small interfering RNA.

One-way ANOVA was used for comparisons among groups, followed by Tukey's post hoc test.  $P < 0.05$  was considered to indicate a statistically significant difference.

## Results

*GADD45A silencing alleviates pathological injury of myocardial I/R.* Results obtained from RT-qPCR and western blotting revealed that GADD45A mRNA and protein expression levels,

respectively, of the I/R group were significantly elevated compared with those in the Control group (Fig. 1A and B). TTC staining results showed that I/R induction significantly increased the size of the ischemic area in rats compared with the Control group (Fig. 1C and D). In addition, the levels of CK and LDH were significantly higher in the I/R group compared with those in the Control group (Fig. 1E and F).

To assess the role of GADD45A in I/R induction, GADD45A silencing was induced by intramyocardial

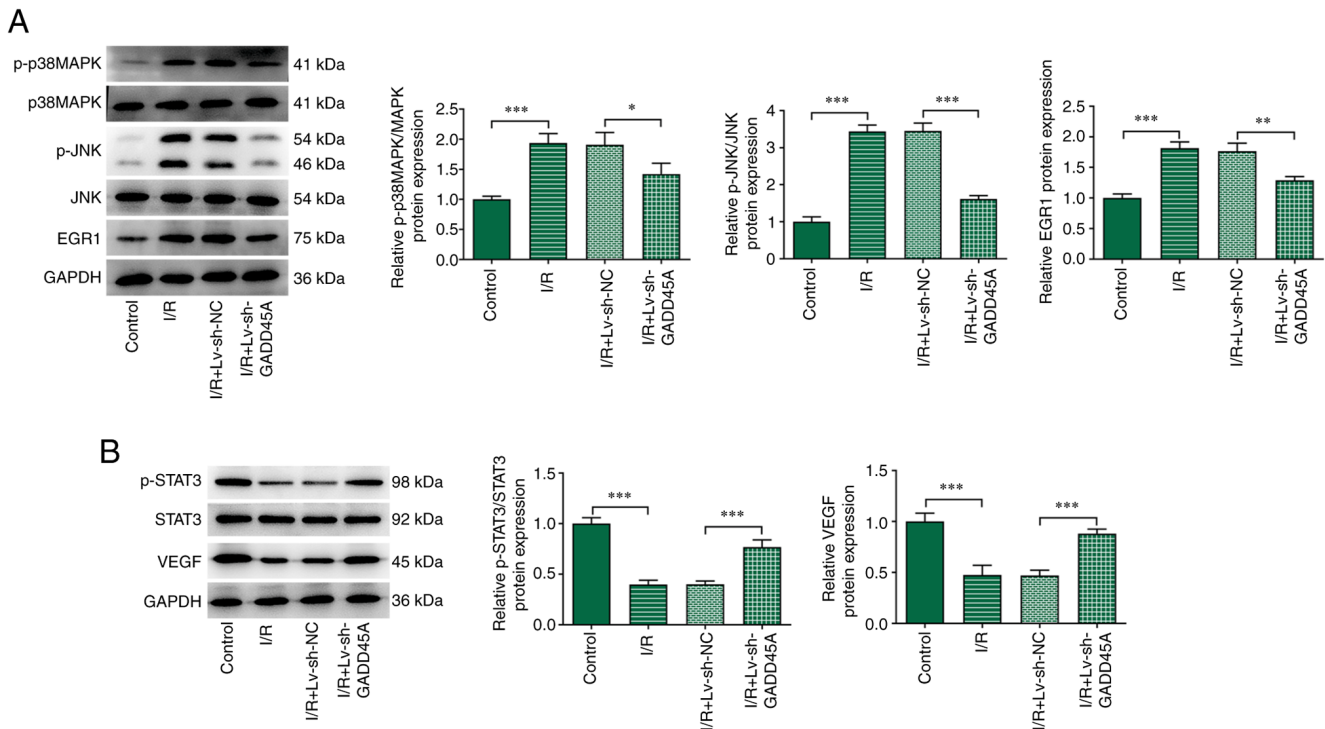


Figure 4. Effects of GADD45A on p38 MAPK/JNK and STAT3/VEGF *in vivo*. (A) p-p38 MAPK, p38 MAPK, p-JNK, JNK, MAPK and EGR1 protein expression levels were examined by western blotting in I/R model rats with or without Lv-si-GADD45A treatment. (B) p-STAT3, STAT3 and VEGF protein expression levels as determined by western blotting. Each experiment was repeated at least three times. \* $P < 0.05$ , \*\* $P < 0.01$ , \*\*\* $P < 0.001$ . EGR1, early growth response 1; GADD45A, growth arrest and DNA damage-inducible  $\alpha$ ; I/R ischemia/reperfusion; Lv, lentivirus; NC, negative control; p-, phosphorylated; si, small interfering RNA.

injection of Lv-si-GADD45A. GADD45A level was successfully decreased following Lv-si-GADD45A induction in I/R model rats compared with that in I/R + Lv-si-NC group (Fig. 2A and B). The sizes of the infarcted area were significantly decreased by GADD45A silencing compared with those in the I/R + Lv-si-NC group (Fig. 2C and D). In the Control group rats, no changes in myocardial tissue were observed, whereas myocardial fibers were disordered with nuclear splitting, edema and enlarged myocardial spaces after I/R induction (Fig. 2E). Myocardial fiber arrangement disorder and interstitial edema were improved in I/R + Lv-si-GADD45A group rats compared with those in I/R + Lv-si-NC group rats (Fig. 2E). In addition, the levels of CK and LDH in the serum were significantly decreased in I/R + Lv-si-GADD45A rats compared with those in the I/R + Lv-si-NC group (Fig. 2F and G).

**GADD45A silencing alleviates loss of vascular endothelial cells in myocardial I/R.** To assess the effect of GADD45A on the loss of vascular endothelial cells, the cells were stained with CD31 and TUNEL. The data showed that I/R induction contributed to increased apoptotic level and decreased CD31 staining compared with the Control group (Fig. 3A); these effects were reversed by GADD45A silencing. The protein expression levels of CD31 and p-eNOS were significantly downregulated, whereas that of ET-1 was upregulated in the I/R group compared with those in the Control group (Fig. 3B); however, GADD45A silencing significantly reversed this effect. In addition, the significantly decreased expression of NO following I/R was partially reversed in I/R model rats treated with si-GADD45A (Fig. 3C). These results demonstrated that

GADD45A silencing may ameliorate the injury induced by myocardial I/R.

**GADD45A silencing inactivates JNK/p38 MAPK signaling and activates STAT3/VEGF signaling in myocardial I/R injured tissues.** To assess the regulatory role of GADD45A in I/R, the protein expression levels of p-p38 MAPK, p38 MAPK, p-JNK, JNK, EGR1, p-STAT3, STAT3 and VEGF were determined. The levels of p-p38 MAPK, p-JNK and EGR1 were significantly increased by I/R induction compared with those in the Control group, and these were subsequently decreased following GADD45A silencing (Fig. 4A). Furthermore, the expression levels of p-STAT3 and VEGF were significantly decreased in the I/R group compared with the Control group (Fig. 4B); these effects were significantly reversed in the I/R + Lv-si-GADD45A group compared with rats in the I/R + Lv-si-NC group.

**GADD45A silencing inhibits p38 MAPK/JNK signaling and activates STAT3/VEGF signaling in H/R-induced CMECs.** To examine the mechanism by which GADD45A is involved in H/R-induced CMEC injury *in vitro*, the cells were subjected to H/R induction. H/R treatment significantly increased GADD45A mRNA and protein expression levels compared with those in the untreated Control group (Fig. 5A and B, respectively). Next, the effects of GADD45A silencing on CMECs were examined. RT-qPCR and western blotting analysis confirmed that GADD45A mRNA and protein expression levels, respectively, were successfully reduced following transfection with siRNA-GADD45A-1 and siRNA-GADD45A-2 compared with siRNA-NC transfection (Fig. 5C and D).

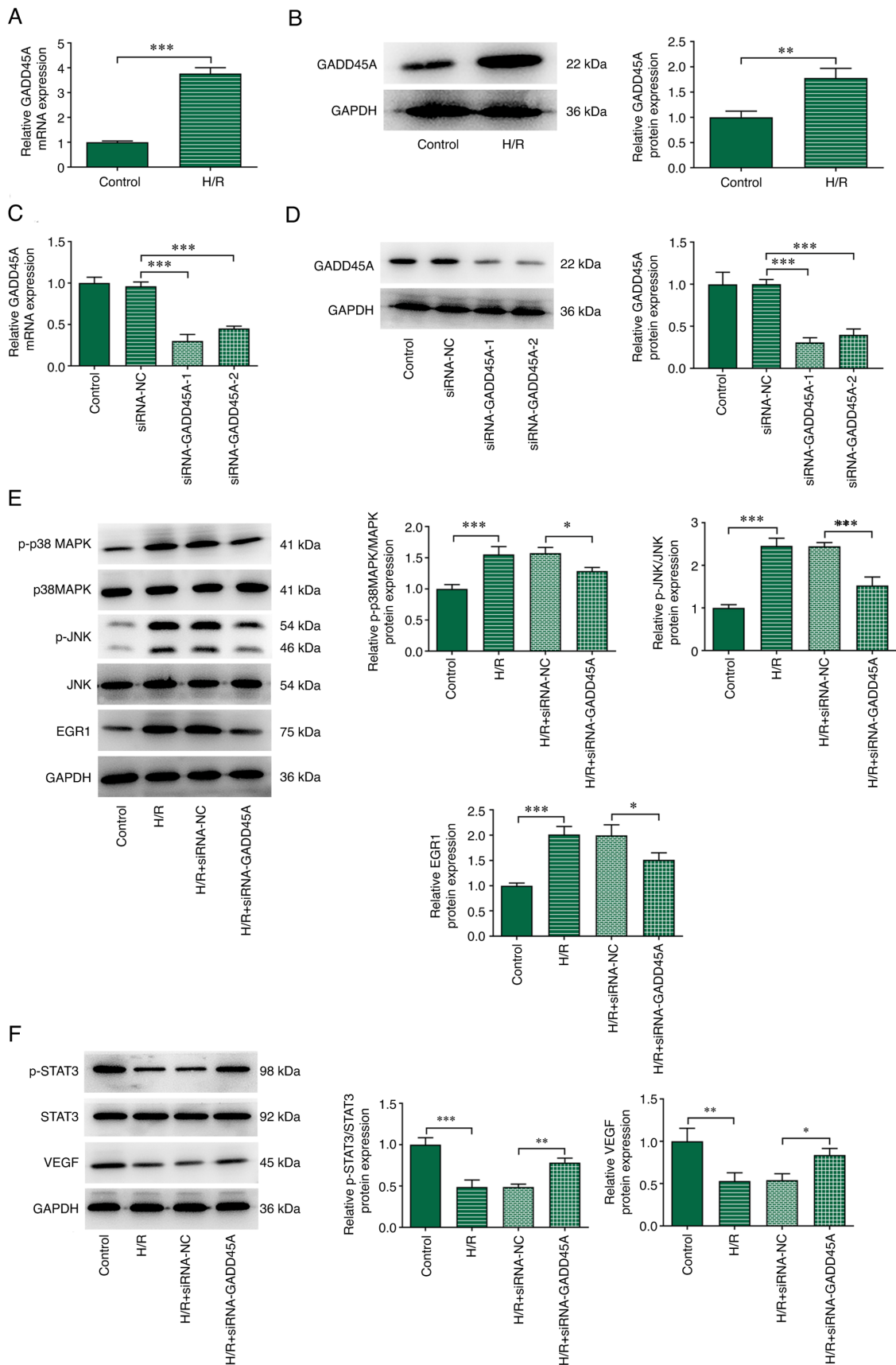


Figure 5. Effects of GADD45A on p38 MAPK/JNK and STAT3/VEGF *in vitro*. CMECs were transfected siRNA-GADD45A-1, siRNA-GADD45A-2 or siRNA-NC for 24 h and then subjected to H/R treatment. (A) mRNA and (B) protein expression levels of GADD45A expression in H/R-induced CMECs. (C) mRNA and (D) protein expression levels of GADD45A expression in CMECs following transfection with siRNA-GADD45A. (E) p-p38 MAPK, p38 MAPK, p-JNK, JNK and EGR1 protein expression levels were determined by western blotting. (F) p-STAT3, STAT3 and VEGF expression levels were determined by western blotting. Each experiment was repeated at least three times. \* $P < 0.05$ , \*\* $P < 0.01$ , \*\*\* $P < 0.001$ . CMEC, cardiac microvascular endothelial cells; EGR1, early growth response 1; GADD45A, growth arrest and DNA damage-inducible  $\alpha$ ; H/R, hypoxia/reoxygenation; NC, negative control; p-, phosphorylated; siRNA, small interfering RNA.

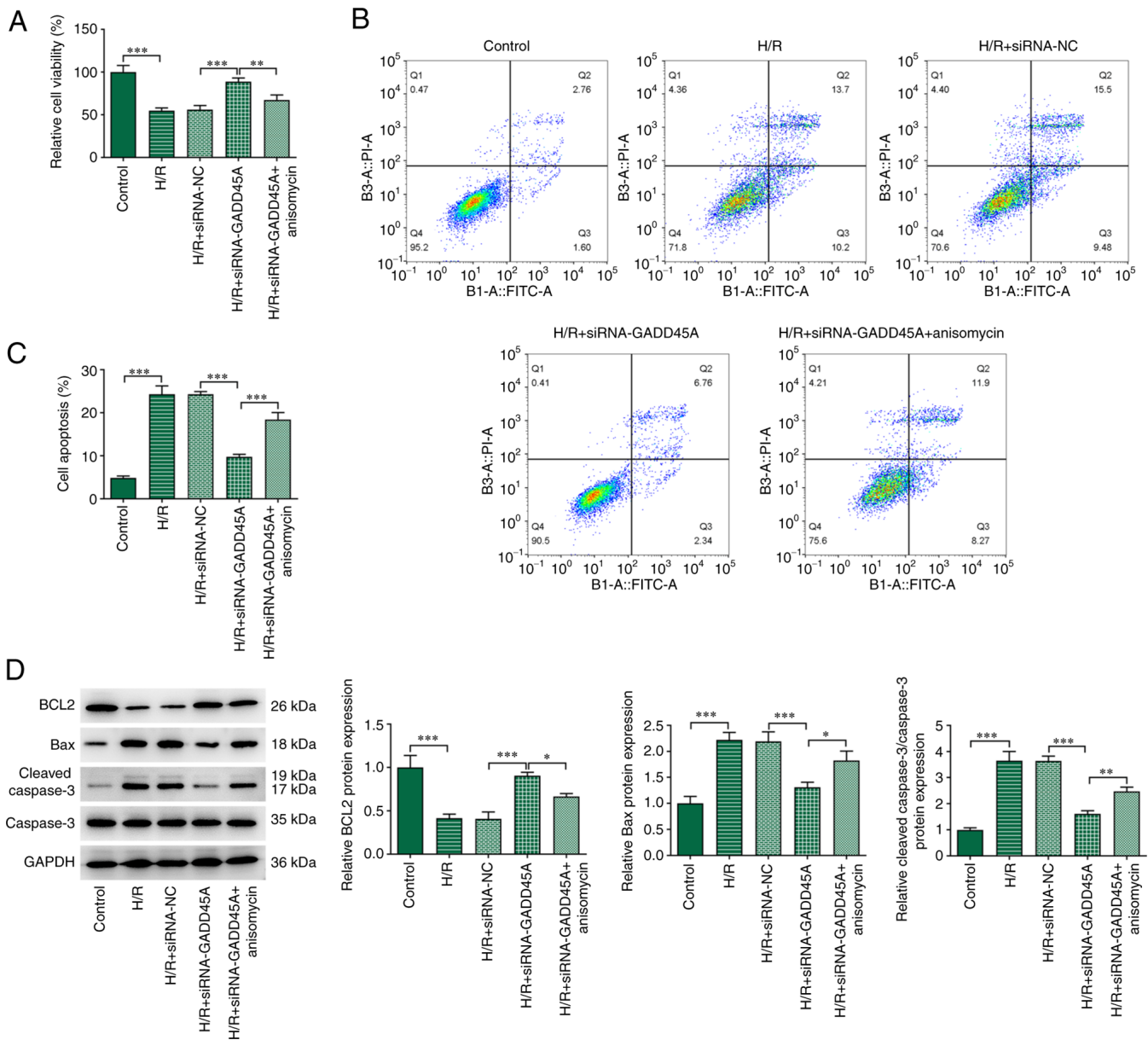


Figure 6. Effects of GADD45A on cell viability and apoptosis of CMEC via the JNK/p38 MAPK signaling pathway. (A) Cell viability was determined by Cell Counting Kit-8 assay in CMECs. (B and C) Apoptotic rates were determined by flow cytometry. (D) Protein expression levels of BCL2, Bax, cleaved caspase 3 and caspase 3 were determined by western blotting analysis. Each experiment was repeated at least three times. \* $P < 0.05$ , \*\* $P < 0.01$ , \*\*\* $P < 0.001$ . CMEC, cardiac microvascular endothelial cells; GADD45A, growth arrest and DNA damage-inducible  $\alpha$ ; H/R, hypoxia/reoxygenation; NC, negative control; siRNA, small interfering RNA.

Based on the transfection efficiency, siRNA-GADD45A-1 was selected for use in subsequent experiments. H/R stimulation activated p38 MAPK/JNK signaling and suppressed STAT3/VEGF signaling, as shown by the increased levels of p-p38 MAPK and p-JNK (Fig. 5E), and the decreased levels of p-STAT3 and VEGF in H/R group (Fig. 5F). In addition, EGR1 expression was increased compared with the Control group (Fig. 5E). GADD45A silencing reversed the effects of H/R induction on these protein expression levels (Fig. 5E and F).

*GADD45A silencing increases viability and reduces apoptosis in H/R-induced CMECs through MAPK and ameliorates angiogenesis through STAT3/VEGF.* The mechanisms by which GADD45A may affect the injury and apoptosis of

CMECs induced by H/R were investigated. H/R induction diminished cell viability and promoted apoptosis (Fig. 6A-C). The knockdown of GADD45A subsequently increased the viability and decreased the apoptosis of H/R-induced CMECs. To verify that GADD45A modulated viability and apoptosis in H/R-treated CMECs via JNK/p38 MAPK signaling, NK and p38 activator anisomycin was used here. Treatment with anisomycin significantly reduced these effects. The declined BCL2 expression and the elevated Bax and Cleaved caspase 3/caspase 3 expressions in the H/R group were all reversed by GADD45A silencing (Fig. 6D). Furthermore, anisomycin treatment also reduced BCL2 protein expression but raised the expression levels of Bax and cleaved caspase 3 in CMECs subjected to H/R + siRNA-GADD45A.

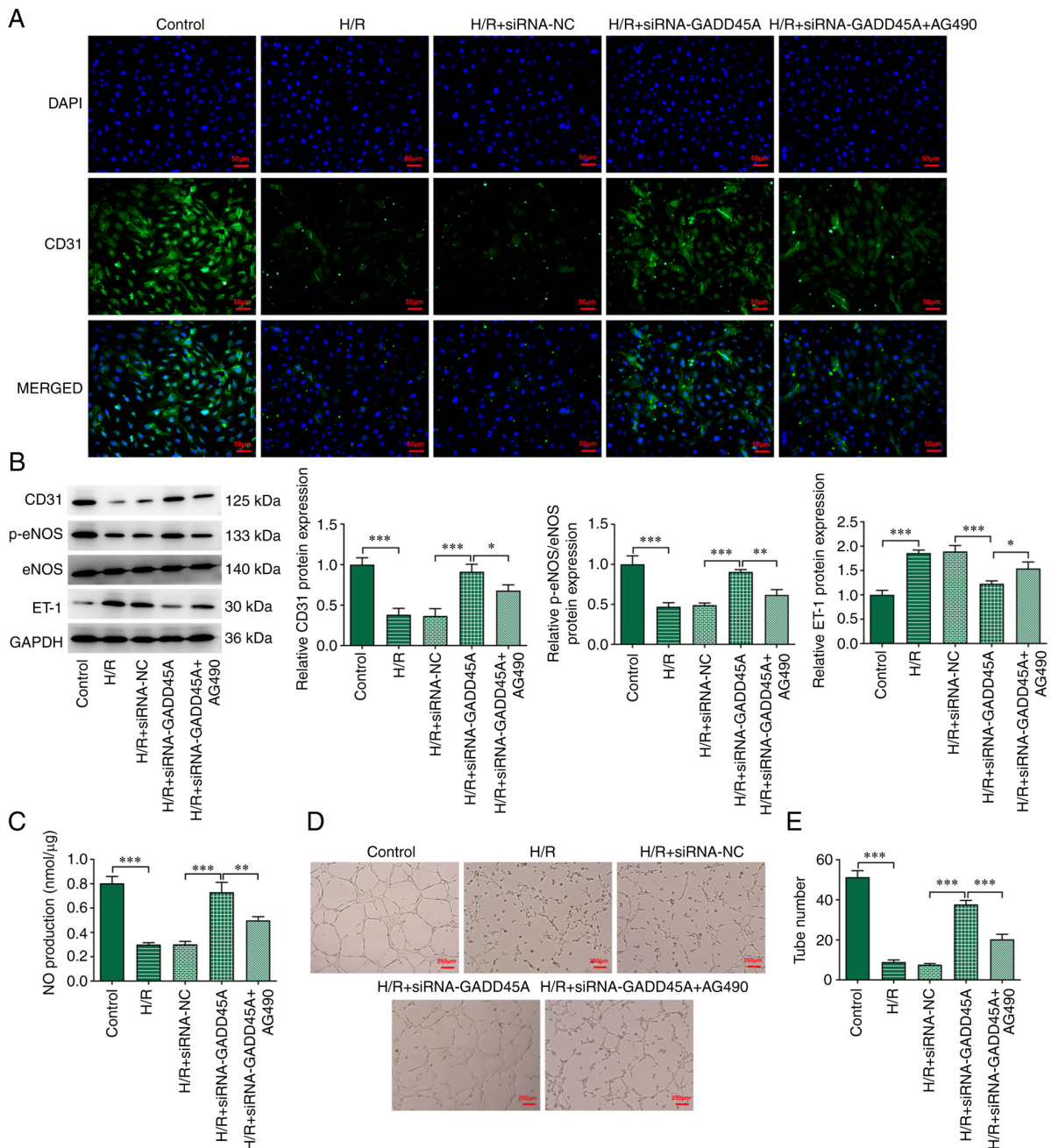


Figure 7. Effects of ATF6 on angiogenesis of CMECs via the STAT3/VEGF signaling pathway. (A) Immunofluorescence staining for CD31 in CMECs; DAPI was used to stain the nucleus. (B) Protein expression levels of CD31, p-eNOS, eNOS and ET-1 were determined by western blotting analysis. (C) NO serum levels were determined using an NO kit. (D and E) Angiogenesis tube formation assay. Each experiment was repeated at least three times. \* $P<0.05$ , \*\* $P<0.01$ , \*\*\* $P<0.001$ . CMEC, cardiac microvascular endothelial cell; eNOS, endothelial NO synthase; ET-1, endothelin-1; GADD45A, growth arrest and DNA damage-inducible  $\alpha$ ; H/R, hypoxia/reoxygenation; NC, negative control; NO, nitric oxide; p-, phosphorylated; siRNA, small interfering RNA.

AG490 is an inhibitor of STAT3 phosphorylation, which may enhance myocardial cell apoptosis and eliminate the protective effect of ischemic pre-conditioning and ischemic post-conditioning in the heart (17). The decreased CD31 expression caused by H/R induction was elevated following GADD45A silencing (Fig. 7A and B); however, AG490 treatment partially reversed this effect. The decreased protein expression levels of CD31 and p-eNOS (Fig. 7B), as well as the reduction in NO (Fig. 7C), in H/R-induced CMECs were significantly increased in H/R + siRNA-GADD45A cells, which were then reduced by AG490 treatment; ET-1 expression exhibited the opposite trend. In the angiogenesis assay,

fewer tubes were observed in the H/R group compared with the Control group, whereas the number of tubes was significantly increased in H/R cells transfected with siRNA-GADD45A (Fig. 7D and E); H/R + siRNA-GADD45A cells treated with AG490 formed fewer tubes compared with the untreated H/R + siRNA-GADD45A group.

## Discussion

As a member of the GADD45 family, which is a group of stress sensors, GADD45A serves a crucial regulatory role in various cellular functions, such as DNA repair,

cell cycle regulation and senescence, and genotoxic stress response (18). Importantly, GADD45A has been reported to be upregulated in myocardial infarction, as shown in I/R injury rat models (12). In addition, GADD45A was able to inhibit proliferation and promote apoptosis in H/R-induced cardiomyocyte injury (12). In the present study, it was shown that GADD45A silencing decreased the size of the myocardial infarcted area, improved myocardial pathological injury and decreased the loss of vascular endothelial cells, demonstrating that the targeting of GADD45A may serve a protective role against I/R-induced injury. Expression of the angiogenesis-related protein CD31 was significantly decreased in the I/R model rats, indicating that a severe infarction occurred to the blood vessels. However, this effect was significantly reduced by GADD45A silencing, which suggested a protective role of GADD45A knockdown against the infarction of blood vessels. Additionally, GADD45A silencing increased CD31 expression and eNOS phosphorylation, as well as decreasing the expression of vascular constriction factor ET-1. Endothelium-generated eNOS is known to be involved in microvascular relaxation and contraction (19). The ratio of eNOS and ET-1 also participates in luminal stenosis and vascular wall edema induced by I/R (20). Thus, I/R induction resulted in myocardial injury by GADD45A, possibly by regulating the eNOS and ET-1.

The present study provided evidence supporting the newly recognized role of GADD45A in ameliorating I/R-induced injury by regulating the MAPK and STAT3/VEGF signaling pathways. Previous studies have shown that GADD45A could activate downstream JNK and p38 signaling proteins, and its silencing suppressed the expression of JNK and p38 (12,21,22). In addition, data from a previous study suggested that I/R could upregulate the levels of JNK and p38 MAPK phosphorylation in CMECs (23), and the activation of JNK and MAPK signals was involved in endothelial cell apoptosis (23). In addition, results from the present study demonstrated that ERK1/2, JNK and p38 inhibitors downregulated EGR1 expression in H/R-induced CMECs at various levels. However, MAPK activators have the opposite effect on EGR1 expression, suggesting that ERK1/2, JNK and p38 are upstream signaling proteins that induce EGR1 (24). The transcription factor EGR1 is known to serve an important role in the pathophysiological damage of a variety of cardiovascular diseases, including atherosclerosis and cardiac hypertrophy (25). Previous studies established that upregulation of EGR1 in the heart induced inflammation after I/R injury (26), and the subsequent use of EGR1 targeting DNazymes reduced infarct size and inflammatory marker production in rodent and pig models (27,28). One study reported that GADD45A could inhibit the expression of STAT3 signaling protein (29), and STAT3 played an important role in cell survival (29). STAT3 is required for the growth of myocardial capillaries after ischemic injury, and loss of STAT3 in myocardial cells leads to reduced capillarization in the left ventricle (30). By contrast, heart-specific STAT3 activation promotes cardiac vascular formation, and JAK/STAT3 and ERK pathways are activated in angiogenesis and NO accumulation in human umbilical vein endothelial cells (30,31).

The present study showed that I/R promoted GADD45A expression, which may subsequently activate the p38

MAPK/JNK pathway to inhibit cell viability and promote apoptosis, as well as to suppress the STAT3/VEGF pathway to affect cell function in CMECs. In summary, this research may provide novel insights into the mechanism and therapy of ischemic cardiomyopathy.

## Acknowledgements

Not applicable.

## Funding

The study was supported by The Clinical Medicine Center for Cardiovascular Disease of Yunnan Province (grant no. ZX2019-08-01).

## Availability of data and materials

The datasets used and/or analyzed during the current study are available from the corresponding author on reasonable request.

## Authors' contributions

YL designed the study. YW, HG and XC performed the research. YW, ZL, YK and YJ analyzed the data. YW wrote the manuscript, which was revised by YL. All authors contributed to editorial changes in the manuscript. All authors read and approved the final manuscript. YL and YW confirm the authenticity of all the raw data.

## Ethics approval and consent to participate

Animal experiments were approved by the Animal Care and Ethics Committee of Yan'an Hospital Affiliated to Kunming Medical University (Kunming, China).

## Patient consent for publication

Not applicable.

## Competing interests

The authors declare that they have no competing interests.

## References

1. Zhou H, Zhang Y, Hu S, Shi C, Zhu P, Ma Q, Jin Q, Cao F, Tian F and Chen Y: Melatonin protects cardiac microvasculature against ischemia/reperfusion injury via suppression of mitochondrial fission-VDAC1-HK2-mPTP-mitophagy axis. *J Pineal Res* 63: e12413, 2017.
2. Mezzaroma E, Toldo S, Farkas D, Seropian IM, Van Tassell BW, Salloum FN, Kannan HR, Menna AC, Voelkel NF and Abbate A: The inflammasome promotes adverse cardiac remodeling following acute myocardial infarction in the mouse. *Proc Natl Acad Sci USA* 108: 19725-19730, 2011.
3. Perrier S, Kindo M, Gerelli S and Mazzucotelli JP: Coronary artery bypass grafting or percutaneous revascularization in acute myocardial infarction? *Interact Cardiovasc Thorac Surg* 17: 1015-1019, 2013.
4. Wu X, Rebolli MR, Korf-Klingebiel M and Wollert KC: Angiogenesis after acute myocardial infarction. *Cardiovasc Res* 117: 1257-1273, 2021.

5. Erbs S, Linke A, Schachinger V, Assmus B, Thiele H, Diederich KW, Hoffmann C, Dimmeler S, Tonn T, Hambrecht R, *et al*: Restoration of microvascular function in the infarct-related artery by intracoronary transplantation of bone marrow progenitor cells in patients with acute myocardial infarction: The doppler substudy of the reinfusion of enriched progenitor cells and infarct remodeling in acute myocardial infarction (REPAIR-AMI) trial. *Circulation* 116: 366-374, 2007.
6. Olivetti G, Ricci R, Beghi C, Guideri G and Anversa P: Response of the border zone to myocardial infarction in rats. *Am J Pathol* 125: 476-483, 1986.
7. Molyneux CA, Glyn MC and Ward BJ: Oxidative stress and cardiac microvascular structure in ischemia and reperfusion: The protective effect of antioxidant vitamins. *Microvasc Res* 64: 265-277, 2002.
8. Cui H, Li X, Li N, Qi K, Li Q, Jin C, Zhang Q, Jiang L and Yang Y: Induction of autophagy by Tongxinluo through the MEK/ERK pathway protects human cardiac microvascular endothelial cells from hypoxia/reoxygenation injury. *J Cardiovasc Pharmacol* 64: 180-190, 2014.
9. Leucker TM, Bienengraeber M, Muravyeva M, Baotic I, Weihrauch D, Brzezinska AK, Warltier DC, Kersten JR and Pratt PF Jr: Endothelial-cardiomyocyte crosstalk enhances pharmacological cardioprotection. *J Mol Cell Cardiol* 51: 803-811, 2011.
10. Zhong J, Ouyang H, Sun M, Lu J, Zhong Y, Tan Y and Hu Y: Tanshinone IIA attenuates cardiac microvascular ischemia-reperfusion injury via regulating the SIRT1-PGC1 $\alpha$ -mitochondrial apoptosis pathway. *Cell Stress Chaperones* 24: 991-1003, 2019.
11. Bai J, Wang Q, Qi J, Yu H, Wang C, Wang X, Ren Y and Yang F: Promoting effect of baicalin on nitric oxide production in CMECs via activating the PI3K-AKT-eNOS pathway attenuates myocardial ischemia-reperfusion injury. *Phytomedicine* 63: 153035, 2019.
12. Liu C, Liu H, Sun Q and Zhang P: MicroRNA 1283 alleviates cardiomyocyte damage caused by hypoxia/reoxygenation via targeting GADD45A and inactivating the JNK and p38 MAPK signaling pathways. *Kardiol Pol* 79: 147-155, 2021.
13. Pontén F, Jirstrom K and Uhlen M: The human protein atlas-a tool for pathology. *J Pathol* 216: 387-393, 2008.
14. Hung YC, Kuo YJ, Huang SS and Huang TF: Trimucrin, an Arg-Gly-Asp containing disintegrin, attenuates myocardial ischemia-reperfusion injury in murine by inhibiting platelet function. *Eur J Pharmacol* 813: 24-32, 2017.
15. Qiu Y, Wu Y, Meng M, Luo M, Zhao H, Sun H and Gao S: GYY4137 protects against myocardial ischemia/reperfusion injury via activation of the PHLPP-1/Akt/Nrf2 signaling pathway in diabetic mice. *J Surg Res* 225: 29-39, 2018.
16. Livak KJ and Schmittgen TD: Analysis of relative gene expression data using real-time quantitative PCR and the 2(-Delta Delta C(T)) method. *Methods* 25: 402-408, 2001.
17. Lei S, Su W, Xia ZY, Wang Y, Zhou L, Qiao S, Zhao B, Xia Z and Irwin MG: Hyperglycemia-induced oxidative stress abrogates remifentanyl preconditioning-mediated cardioprotection in diabetic rats by impairing caveolin-3-modulated PI3K/Akt and JAK2/STAT3 signaling. *Oxid Med Cell Longev* 2019: 9836302, 2019.
18. Salvador JM, Brown-Clay JD and Fornace AJ Jr: Gadd45 in stress signaling, cell cycle control, and apoptosis. *Adv Exp Med Biol* 793: 1-19, 2013.
19. Wang J, Toan S and Zhou H: New insights into the role of mitochondria in cardiac microvascular ischemia/reperfusion injury. *Angiogenesis* 23: 299-314, 2020.
20. Li C, Ma Q, Toan S, Wang J, Zhou H and Liang J: SERCA overexpression reduces reperfusion-mediated cardiac microvascular damage through inhibition of the calcium/MCU/mPTP/necroptosis signaling pathways. *Redox Biol* 36: 101659, 2020.
21. Li FH, Han N, Wang Y and Xu Q: Gadd45a knockdown alleviates oxidative stress through suppressing the p38 MAPK signaling pathway in the pathogenesis of preeclampsia. *Placenta* 65: 20-28, 2018.
22. Tront JS, Hoffman B and Liebermann DA: Gadd45a suppresses Ras-driven mammary tumorigenesis by activation of c-Jun NH2-terminal kinase and p38 stress signaling resulting in apoptosis and senescence. *Cancer Res* 66: 8448-8454, 2006.
23. Yu F, Liu Y and Xu J: Pro-BDNF contributes to hypoxia/reoxygenation injury in myocardial microvascular endothelial cells: Roles of receptors p75<sup>NTR</sup> and sortilin and activation of JNK and caspase 3. *Oxid Med Cell Longev* 2018: 3091424, 2018.
24. Lu S, Zhang Y, Zhong S, Gao F, Chen Y, Li W, Zheng F and Shi G: N-n-butyl haloperidol iodide protects against hypoxia/reoxygenation injury in cardiac microvascular endothelial cells by regulating the ROS/MAPK/Egr-1 pathway. *Front Pharmacol* 7: 520, 2017.
25. Khachigian LM: Early growth response-1 in cardiovascular pathobiology. *Circ Res* 98: 186-191, 2006.
26. Bhindi R, Khachigian LM and Lowe HC: DNazymes targeting the transcription factor Egr-1 reduce myocardial infarct size following ischemia-reperfusion in rats. *J Thromb Haemost* 4: 1479-1483, 2006.
27. Bhindi R, Fahmy RG, McMahon AC, Khachigian LM and Lowe HC: Intracoronary delivery of DNazymes targeting human EGR-1 reduces infarct size following myocardial ischemia reperfusion. *J Pathol* 227: 157-164, 2012.
28. Rayner BS, Figtree GA, Sabaretnam T, Shang P, Mazhar J, Weaver JC, Lay WN, Witting PK, Hunyor SN, Grieve SM, *et al*: Selective inhibition of the master regulator transcription factor Egr-1 with catalytic oligonucleotides reduces myocardial injury and improves left ventricular systolic function in a preclinical model of myocardial infarction. *J Am Heart Assoc* 2: e000023, 2013.
29. Yang F, Zhang W, Li D and Zhan Q: Gadd45a suppresses tumor angiogenesis via inhibition of the mTOR/STAT3 protein pathway. *J Biol Chem* 288: 6552-6560, 2013.
30. Hilfiker-Kleiner D, Hilfiker A, Fuchs M, Kaminski K, Schaefer A, Schieffer B, Hillmer A, Schmiedl A, Ding Z, Podewski E, *et al*: Signal transducer and activator of transcription 3 is required for myocardial capillary growth, control of interstitial matrix deposition, and heart protection from ischemic injury. *Circ Res* 95: 187-195, 2004.
31. Osugi T, Oshima Y, Fujio Y, Funamoto M, Yamashita A, Negoro S, Kunisada K, Izumi M, Nakaoka Y, Hirota H, *et al*: Cardiac-specific activation of signal transducer and activator of transcription 3 promotes vascular formation in the heart. *J Biol Chem* 277: 6676-6681, 2002.



This work is licensed under a Creative Commons Attribution-NonCommercial-NoDerivatives 4.0 International (CC BY-NC-ND 4.0) License.